Case Studies in Construction Materials 16 (2022) e01022

Contents lists available at ScienceDirect

Case Studies in Construction Materials

journal homepage: www.elsevier.com/locate/cscm

Web crippling behaviour of cold-formed high-strength steel unlipped channel beams under End-One-Flange load case

Elilarasi Kanthasamy [a,*], Dinesh Lakshmanan Chandramohan [b], Gunalan Shanmuganathan [c], Keerthan Poologanathan [a], Perampalam Gatheeshgar [d], Marco Corradi [a], Alex Mcintosh [a]

[a] Department of Mechanical and Construction Engineering, Northumbria University, Newcastle upon Tyne, UK
[b] Anna University, Chennai 600025, India
[c] School of Engineering and Built Environment, Griffith University, Australia
[d] School of Computing, Engineering & Digital Technologies, Teesside University, Middlesbrough, UK

ARTICLE INFO

Keywords:
High-strength cold-formed steel
Unlipped channel section
Web crippling
End-One-Flange (EOF) load case
Finite element analysis
Direct strength method

ABSTRACT

High-strength Cold-Formed Steel (CFS) members are widely adopted as structural members in building structures due to its higher ultimate capacity. The flexural members are often subjected to concentrated transverse loads which may leads to buckling instabilities including web crippling. However, there is no appropriate design rules and studies are available to estimate the web crippling strength of high-strength CFS members. Hence, this paper presents a detailed numerical investigation on high-strength CFS unlipped channel sections subjected to End-One-Flange (EOF) loading condition with nominal yield strengths of 700 MPa, 900 MPa and 1000 MPa. For numerical simulation study, non-linear Finite Element (FE) models were developed and validated with the experimental results followed by an extensive parametric study using ABAQUS. In total, 243 FE models were developed with different geometric and material parameters including section thickness, material strength, web slenderness ratio, inside bent radius to thickness ratio and bearing length to thickness ratio. The ultimate web crippling strength results were compared with the available design guidelines to check their suitability and accuracy in terms of strength prediction. Then, new design rules to predict the web crippling capacity of high-strength CFS unlipped channel section under EOF condition based on unified and Direct Strength Method (DSM) approaches were proposed.

1. Introduction

In recent years, applications of the high-strength cold-formed steel have been predominant in the construction industry due to its inherent advantages over the conventional strength steel sections such as high strength to weight ratio, material saving, handling and transportation cost, suitable for long-span and high-rise building structures and lesser carbon footprint [1]. The nominal yield strength of the CFS with high-strength materials range from 460 MPa to 1100 MPa are commercially available in the market [2,3].

High-strength CFS structural members are often subjected to concentrated transverse load or localised load or support reactions which may cause web crippling failure. According to AISI S909 [4], web crippling failure is categorised into four main types based on

* Corresponding author.
E-mail address: elilarasi.kanthasamy@northumbria.ac.uk (E. Kanthasamy).

https://doi.org/10.1016/j.cscm.2022.e01022
Received 22 December 2021; Received in revised form 15 March 2022; Accepted 18 March 2022
Available online 22 March 2022

the location of the load and support conditions: Interior-One-Flange (IOF), End-One-Flange (EOF), Interior-Two-Flange (ITF) and End-Two-Flange (EOF) loading. The load case is considered to as end load where failure occurs within the $1.5d_1$ from the end distance and if the failure occurs higher than the $1.5d_1$ from the end distance is referred as interior loading. Similarly, one-flange and two-flange loading conditions are referred as the clear distance between the edges of the bearing plates is higher than the $1.5d_1$ and lesser than the $1.5d_1$, respectively. Where d_1 is clear web height of the sections (Fig. 1).

Theoretical investigation of the web crippling capacity is complicated due to non-uniform stress distribution, yielding near the localised area, inelastic behaviour and initial imperfection of web element [4]. Since the 1940 s, many researchers have performed experimental investigations on the web crippling behaviour of CFS sections. Prabakaran and Schuster [6] carried out extensive web crippling strength data analysis and developed an appropriate design equation to predict the web crippling capacity of the CFS sections based on more than 1200 experimental test data that comprised the results of I section, Z-sections, Channel sections and multiple web sections. Later, this study was extended by Beshara and Schuster [7] and they proposed improved web crippling coefficients which was adopted in the North American Specification (NAS) [8].

Young and Hancock conducted an experimental investigation on the web crippling behaviour of CFS unlipped channel sections under IOF, EOF, ITF and ETF loading conditions and proposed design equations based on a simple plastic mechanism [9]. Moreover, same authors extended their experimental studies on CFS channel sections with unfastened flange conditions [10] and fastened flange conditions [11] under two-flange web crippling loading conditions. Ren et al. [12] carried out non-linear finite element (FE) analysis of CFS channel sections subjected to one-flange loading conditions, where FE models were validated against the experimental results by Young and Hancock [9] and proposed web crippling design equations for the web slenderness range from 7.8 to 108.5. In addition, Macdonald et al. [13,14] and Chen et al. [15] conducted experimental and numerical investigations on CFS lipped channel sections subjected to all four load cases (IOF, EOF, ITF and ETF), where a wide range of sections dimensions were accommodated. Duarte and Silvestre [16] performed numerical simulation of CFS plain channel beams under concentrated loads and proposed new slenderness-based approach web crippling strength design rules.

Natario et al. [17,18] conducted web crippling investigations on CFS beam sections with fastened and unfastened flange conditions using past experimental research studies and developed new design rules using the DSM based approach to determine web crippling strength under ETF and ITF loading conditions, respectively. To develop DSM approach, the authors performed elastic buckling analysis to determine elastic buckling load and rigid-plastic analyses to calculate the plastic load. In addition, Gunalan and Mahendran carried web crippling studies of CFS unlipped channel sections subjected to two-flange loading conditions [19] and one-flange loading conditions [20], this study compared their experimental results with the available design rules [8,21] and proposed modifications to web crippling coefficients.

Besides, high-strength steel sections are widely adopted as structural members in the building construction due to its architectural advantages and structural performance. However, very limited studies [22–25] investigated the web crippling behaviour of high-strength CFS sections. Santaputra et al. [22] Conducted web crippling studies on brake-pressed CFS hat and built-up sections with yield strengths of the material range from 401 to 1138 MPa. Wu et al. [23] carried out web crippling tests on high-strength CFS hat and deck sections with yield strengths up to 894 MPa and stated low ductility properties of the steel causes a negligible effect on web crippling capacity of the sections. Recently, Li and Young [24] conducted experimental studies on web crippling behaviour of

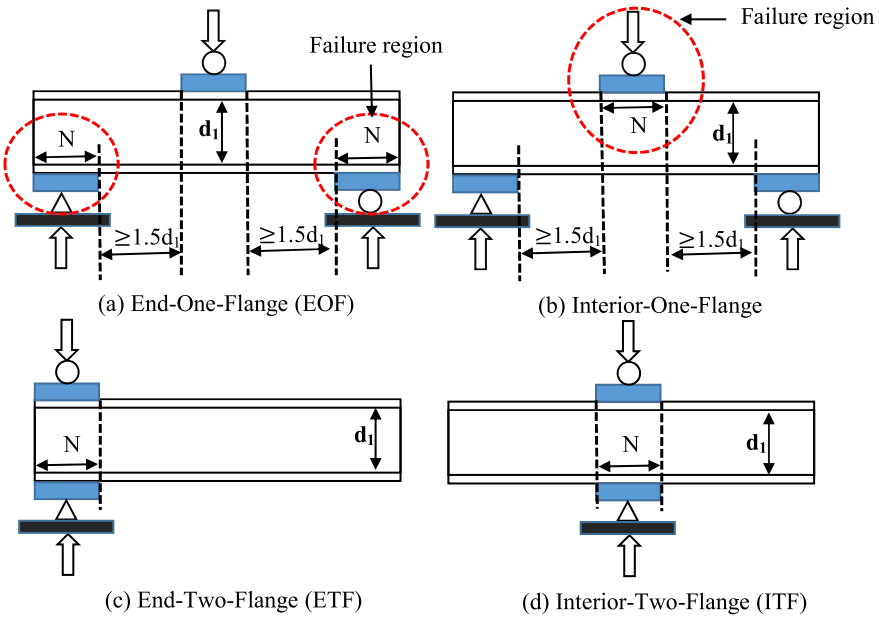

Fig. 1. Four load cases for web crippling failure [5].

high-strength CFS rectangular and square tubular sections under four varying load cases, where the test specimens web slenderness was varied from 8.3 to 35.8 whilst yield strengths of the material were 700 and 900 MPa. Experimental results of this study were compared with the available web crippling design rules and the study reported that the design rules were not suitable to determine the nominal web crippling capacity of the high-strength steel tubular sections. Later, Li and Young [25] performed extensive numerical investigations on high-strength tubular sections subjected to web crippling loading conditions. The improved modified design equation and unified Direct Strength Method (DSM) were prosed based on the results to predict the nominal web crippling strength of high-strength CFS tubular sections. However, web crippling study of CFS channel sections with yield strength greater than 690 MPa has been very limited.

Moreover, Sundararajah et al. [26–29] conducted detailed experimental and numerical simulation investigations on high-strength CFS channel sections under all four web crippling load cases (IOF, ITF, EOF and ETF). To account the effect of different geometrical parameters, their study considered different section lengths, web heights, internal radii, bearing lengths and material strengths. The results were compared with available design guidelines [8,21,30] and proposed new DSM approach equations and proposed modifications to the web crippling coefficients. It should be note that this study performed on high-strength CFS sections with limited up to 550 MPa. To study the fastened flange condition, Janarthanan et al. [31,32] performed the experimental and numerical analysis of web crippling failures of CFS unlipped channel sections under EOF and IOF load cases with fastened flange condition and proposed modifications based on the AISI S100 [8]. In addition, the web crippling investigations were carried on CFS SupaCee sections under one-flange loading conditions [33] and two-flange loading conditions [34] by Sundararajah et al. [33,34]. Recently, Almatrafi et al. [35] performed web crippling investigation on CFS sigma sections under IOF loading condition and developed slenderness based approach method design equation while Gatheeshgar et al. [36], [37] investigated the web crippling behaviour of new generation of staggered slotted perforated channels under one-flange load cases. Besides, it should be noted that some recent studies investigated the effect of web openings on web crippling strength in CFS channel beams [38–44] and hollow flange beams [45].

The aforementioned literature studies and currently available design guidelines for CFS structures such as AISI S100 [8], AS/NZS 4600 [21] and Eurocode 3 Part 1–3 [30] are suitable to estimate the web crippling capacity of CFS sections made of relatively lower steel grades (yield strengths) and there is a necessity to assess the suitability for high-strength CFS sections. However, no research studies investigated the web crippling behaviour of high-strength CFS channel sections. Hence, this research conducted a numerical investigation on web crippling behaviour of high-strength CFS unlipped channel section under EOF loading condition with yield strength ranged from 700 to 1000 MPa. A detailed parametric study was performed with 243 FE models considering different cross-sectional dimensions, section thicknesses, material strengths, bearing lengths and internal radii. The results were compared with the available design equations and suitable design equations and DSM equations to predict the web crippling strength of the high-strength CFS unlipped channel sections subjected to EOF loading condition were developed.

2. Numerical modelling

This part describes the FE model development of high-strength CFS unlipped channel section under EOF web crippling loading condition. In past years, many researches [22,25,27,29,32,46] carried out FE analysis to study the web crippling behaviour of channel sections in detail. ABAQUS 6.14 [47] software is used for numerical modelling. Initially, full and half models were simulated and validated against to the experimental test results which is discussed in Section 3. The results obtained from both full and half models were very similar. Therefore, half model simulation was found to be suitable for parametric study considering lesser time and cost of the analysis.

2.1. Material definition

Material properties of high-strength CFS unlipped channel section was defined in the ABAQUS using (a) density, (b) Young's modulus, (c) Poisson's ratio and (d) stress-strain curve inputs. Density of the CFS was 7850 kg/m^3 whilst Young's modulus and Poisson's ratio were 203,000 MPa and 0.3, respectively. Moreover, Recently Leroy Gardner and Xiang Yun [48] proposed a two-stage Ramberg-Osgood model (Eqs. (1)–(6)) to describe the stress-strain curve of the cold-formed steel which is based upon the material model developed by Mirambell and Real [49] for stainless steel. The researchers [48] gathered a huge collection of the stress-strain models from the literature review by considering various material strengths, shapes and forms of the production such as press braked or cold-rolled and validated. Also, the study [48] suggested that Rossi et al. [50] study can be used to obtain the material model of the corner regions (Eqs. (7)–(10)). Plastic deformation in the corner regions during the manufacturing process causes corner strength enhancement [50]. Corner strength enhancement of high strength steel sections has been derived using Eqs. (7)–(10). Even though stainless steel also adopts corner strength enhancement, notable differences can be observed between applied corner strength curve equations of high strength and stainless steel. The material models proposed by Gardner and Yun [48] and Rossi et al. [50] were applied in this study to find out the stress-strain behaviour of flat and corner regions respectively.

Applied stress-strain relationship of the flat region in this study:

$$\varepsilon = \begin{cases} \frac{f}{E} + 0.002\left(\frac{f}{f_y}\right)^n \\ \frac{f-f_y}{E_{0.2}} + \left(\varepsilon_u - \varepsilon_{0.2} - \frac{f_u - f_y}{E_{0.2}}\right)\left(\frac{f-f_y}{f_u-f_y}\right)^m + \varepsilon_{0.2} \end{cases} \quad (1)$$

The suggested values and expressions for the key input parameters into Eq. (1) are as follows:
n - First strain hardening exponent:

$$n = \frac{\ln(4)}{\ln\left(f_y/\sigma_{0.05}\right)} \quad (2)$$

In this study, the first strain-hardening exponent was taken from following table (Table 1) [50].
$E_{0.2}$ - Tangent modulus of the stress-strain curve at the yield strength (0.2% proof stress):

$$E_{0.2} = \frac{E}{1 + 0.002n\frac{E}{f_y}} \quad (3)$$

ε_u - Strain corresponding to the ultimate tensile strength f_u:

$$\varepsilon_u = 0.6\left(1 - \frac{f_y}{f_u}\right) \quad (4)$$

For an unknown ultimate strength, f_u:

$$f_u \Big/ f_y = 1 + \left(130/f_y\right)^{1.4} \quad (5)$$

m - Second strain-hardening exponent:

$$m = 1 + 3.3\frac{f_y}{f_u} \quad (6)$$

$f_{y,c}$ - Enhanced yield strength of corner regions of cold-rolled or press-braked sections:

$$f_{y,c} = p\left(\varepsilon_{c,av} + \varepsilon_{0.2}\right)^q, but \leq f_u \quad (7)$$

$\varepsilon_{c,av}$ - Averaged plastic strain induced during the forming of the corner regions of press-braked and cold-rolled sections:

$$\varepsilon_{c,av} = \frac{t}{2(2r_i + t)} \quad (8)$$

p and q - Material parameters calculated directly from the basic properties of the unformed material:

$$p = \frac{f_y}{\varepsilon_{0.2}^q} \quad (9)$$

$$q = \frac{\ln\left(f_y/f_u\right)}{\ln\left(\varepsilon_{0.2}/\varepsilon_u\right)} \quad (10)$$

2.2. Element type

The web crippling setup of high-strength CFS unlipped channel section under EOF loading comprises channel beam section, loading plate, supporting plates and web side plates (WSPs). The unlipped channel beam was modelled using 3D deformable shell elements, which is quadrilateral shell S4R element type with linear-four nodes, reduced integration, finite strain and hourglass control. On the other hand, discrete rigid element with four nodded R3D4 was chosen to model the loading plate, bearing plate and WSP to simulate high stiffness and rigidity than the unlipped channel section. The FE model with S4R element type was often used to study web crippling behaviour of CFS sections [22,25,27,29,32,46,51].

Table 1
Strain-hardening exponents [50].

	n	m
Flat coupons	7.6	3.8
Corner coupons	7.0	4.2

2.3. Mesh property

In this study, mesh sensitivity analysis was carried to select the proper mesh size for the high-strength CFS beams under EOF load case shown in Fig. 2. The result shows similar observation as previous study [52]. Therefore, based on the past web crippling research studies [27,29,52], mesh size of 5 mm × 5 mm for flat regions and 1 mm × 5 mm for corner regions were adopted for the unlipped channel sections. Finer mesh size in the corner region of the section ensures the proper plastic deformation at the web-flange juncture and appropriate stress distribution between the flange and web of the channel section. The discrete rigid elements including the loading plate, supporting plate and WSPs are not directly associated with the web crippling strength. Therefore, a relatively coarser 10 mm × 10 mm mesh size were considered for the rigid elements, which has no influence in the analysis process. Fig. 3 shows the mesh property of the unlipped channel section subjected to EOF web crippling loading.

2.4. Loading and boundary condition

To simulate suitable boundary conditions to the loading and supporting plates, a reference point was assigned to the respective rigid element. The boundary condition of EOF loading condition was applied through the reference point. Fig. 4 represents the detailed boundary condition of the full and half models under web crippling. Moreover, half model requires symmetry line boundary condition to replicate the full model setup. To simulate exact experimental set-up, translation movement of X and Z direction along with all rotational movement except X direction were restrained at the loading plate (top bearing plate). The vertical displacement of 20 mm was applied through the loading plate in downward Y direction. To create a slower initial stage displacement and develop smooth deformation in the structure, the applied displacement load is controlled by using smooth step amplitude function in ABAQUS. All the translational and rotational movements except rotation about X and Y axes were restricted in the supporting plate (bottom bearing plate). In addition, the symmetry line in the half models were restrained by ZSYMM symmetrical option, where the movements of Z axis and rotation movements in the X and Y direction were not allowed.

2.5. Contact properties

In the FE model, the contact between channel section and the loading and supporting plates were modelled using contact pair interaction option in the ABAQUS. According to past research studies [25,29,32,46], surface-to-surface contact property was created between the sections. To simulate proper interaction properties, rigid plates were defined as master surface whereas slave surface was assigned for respective flat flange and corner radius portion of the beam. The unlipped channel beam section element was modelled by centreline method. Therefore, to ensure the half of the section thickness gap between rigid element and beam section 'face-to-face' position constraint was employed, which restrict the overlaps of two contact surface. The interaction property was defined with the normal and tangential behaviour between the flanges of beam section and the bearing plates. Among various contact formulation, 'hard' contact is adopted for the pressure-overclosure and penalty friction formulation with coefficient of 0.4 was assumed to represent the friction slip during analysis [5,25,27,29,32,36,37,52]. The recent study of Janarthanan et al. [32] suggested that the friction coefficient of value is 0.4 for CFS unlipped channel beams under one-flange load case among consideration of various coefficient values (0–0.8) and stated that the friction coefficient has negligible effect in web crippling strength, which is likely to the study of Natário et al. [53].

2.6. Analysis type

Generally, static and quasi-static problems were able to solve using ABAQUS/Implicit and ABAQUS/ Explicit solver available in ABAQUS [5,52]. For dynamic problems, ABAQUS/Implicit analysis method may cause convergence issues during analysis process while ABAQUS/ Explicit solver is well suited. Therefore, ABAQUS/ Explicit method of approach is used in this study to analysis the

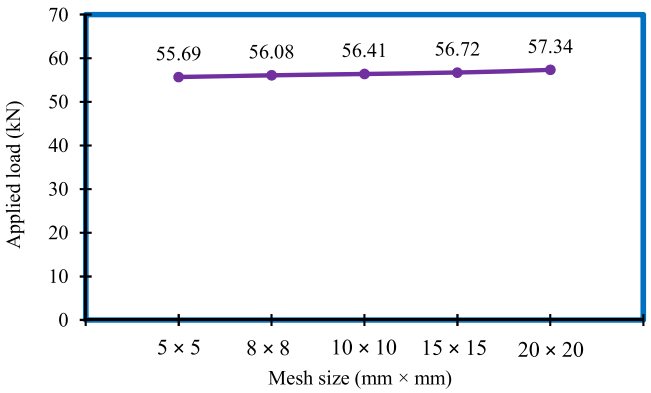

Fig. 2. Mesh sensitivity analysis.

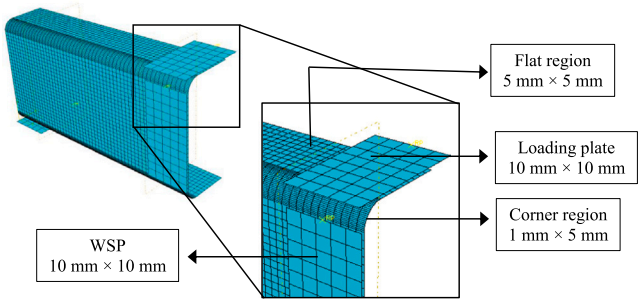

Fig. 3. Mesh property of unlipped channel section.

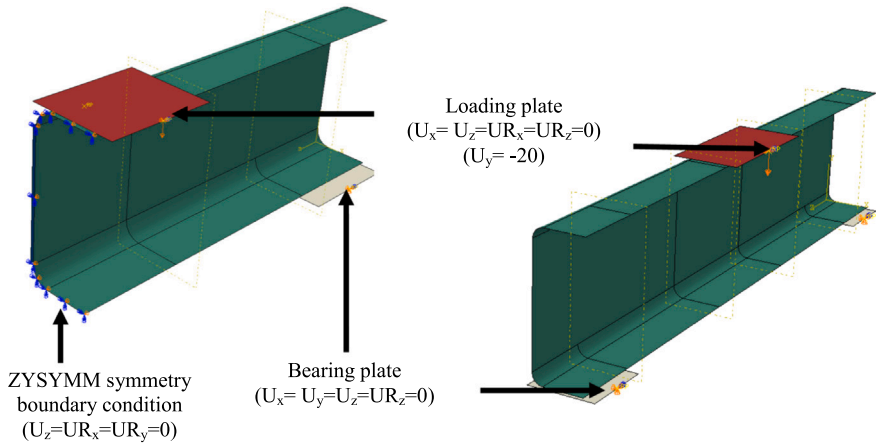

Fig. 4. Assembly and boundary condition of half and full FE models.

web crippling behaviour of high-strength CFS beams. The similar technique was used in the previous studies [5,27,29,52]. Smooth step load rate with step time of 1 s (ST = 1 s) was considered in this study, this is because load rate with small step time (ST = 0.1 s) able to cause higher and irregular failure effect in the result [27,29]. To reduce the computational time, mass scaling option were used in ABAQUS/ Explicit solver while which leads to increase in inertial force and significant changes in the results. Therefore, mass scaling option were not included in this study to perform high accuracy of analysis [27,29,37]. To be noted, Sundararajah et al. [27] conducted detailed investigation on both load rate scaling and mass scaling selection for one-flange load case.

2.7. Initial geometrical imperfections

Past studies predicted that web crippling capacity of CFS will not affect much by not considering the geometric imperfections [29, 38,40,44,45,47,52]. Moreover, Sundararajah et al. [27] and Gatheeshgar et al. [37] studies stated that the effect of geometric

Table 2
Comparison of experimental [24,25] and FE analysis results.

Section	Experimental (kN)	FE Predictions- full model (kN)	Experimental/FE – full model	FE Predictions – half model (kN)	Experimental/FE – half model
H80 × 80 × 4N50	80.5	77.85	1.03	83.85	0.96
H120 × 120 × 4N60	79.2	73.75	1.07	73.18	1.08
H160 × 160 × 4N150	108.5	109.63	0.99	115.98	0.94
H160 × 160 × 4N90	80.0	86.67	0.92	87.67	0.91
H100 × 100 × 4N50–2	73.5	70.95	1.04	69.38	1.06
H100 × 100 × 4N50–3	72.7	69.92	1.04	68.22	1.07
H100 × 100 × 4N30–1	52.0	54.669	0.95	51.59	1.01
H100 × 100 × 4N30–2	49.6	49.90	0.99	51.66	0.96
V100 × 100 × 4N90	109.1	121.07	0.9	118.46	0.92
V100 × 100 × 4N50	72	75.52	0.95	73.36	0.98
Mean			0.99		0.99
COV			0.06		0.06

Note: H is high yield strength steel (700 MPa), V is very high yield strength steel (900 MPa) and N is bearing length.

imperfection on web crippling capacity under one-flange loading condition is less than 3% and 2% respectively. Therefore, geometric imperfection is neglected in the numerical modelling of this study.

2.8. Residual stresses

Effect of residual stress in the web crippling behaviour of CFS are studied by various researchers and stated that effect in web crippling capacity is less than 0.5% [54]. Therefore, residual stress effect was not considered in this study. For high strength steel sections, effect of residual stress is very less compared to the effect of corer strength enhancement. Therefore, corner strength enhancement was considered in this study whilst residual stress was neglected.

3. Validation

A non-linear FE model was developed and validated with the experimental test results [24,25] of the high-strength CFS tubular sections under EOF loading condition to ensure the accuracy and reliability of the numerical simulation. Full model and half model of tubular sections were developed and compared with the experimental results. Both the half and full FE model results showed good agreement with the test results in terms of predicting the ultimate web crippling capacity as shown in Table 2.

In total, 10 web crippling experimental results of high-strength tubular sections including the yield strengths of 700 MPa and 900 MPa were validated using both full and half models which is presented in Table 2. The mean and COV values of both the full and half models were 0.99 and 0.06. Hence, the developed FE models were able to predict the web crippling capacity under EOF condition with high accuracy level.

In addition, the FE model results were validated against the experimental results in terms of applied load vs vertical displacement curve. Fig. 5 shows the load vs vertical displacement curves for the section H120 × 120 × 4N60 from the experimental, FE-full model and FE-half model. Fig. 5 clearly demonstrates that the both FE-full and half model curves have good correlation with the experimental results from the initial loading stage up to post-failure stage. Also, FE-full model and FE-half model results of H120 × 120 × 4N60 show very similar curve.

The failure modes of the numerical model were also compared against with web crippling test results. Figs. 6 and 7 show the comparison of experimental failure modes of section H160 × 160 × 4N90 with the FE-full model and FE-half model, respectively. The failure modes of both numerical models agreed well with the experimental deformation. Meantime, FE-full model and FE-half model showed similar failure modes. Overall, the FE-half model method was satisfactorily in simulating the experimental web crippling ultimate capacity, failure modes and load vs vertical displacement response of high-strength CFS sections under EOF loading condition with less time consumption. Hence, half model was adopted to the parametric study.

4. Parametric study

After a comprehensive validation process, a detailed parametric study was developed to investigate the web crippling behaviour of the high-strength CFS unlipped channel section under EOF loading conditions. Therefore, 243 non-linear FE models were developed with consideration of different geometrical parameters including three section dimensions 150 × 60, 200 × 75, 250 × 85 with section thicknesses (t) of 4 mm, 6 mm and 8 mm. In addition, three material strengths (f_y) of 700 MPa, 900 MPa and 1000 MPa and inside bent radius ranged (r_i) from 12 to 18 mm were taken for this study. Also, three bearing lengths (N) of 50 mm, 100 mm and 150 mm were considered. Moreover, this study has incorporated the effect of web slenderness ratio (d_1/t) ranged from 18.75 to 62.5, inside bent radius to thickness (r_i/t) ranged from 1.5 to 4.5 and bearing length to thickness (N/t) ranged from 6.25 to 37.5 to study the web crippling behaviour. Table 3 shows the detailed parametric study plan and the corresponding section dimensions are illustrated in Fig. 8.

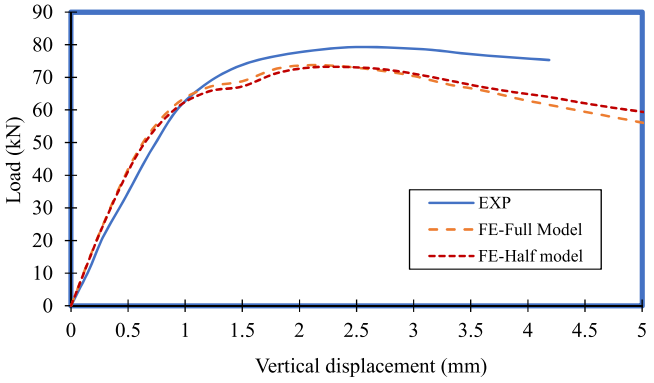

Fig. 5. Applied load vs vertical displacement plot of section H120 × 120 × 4N60.

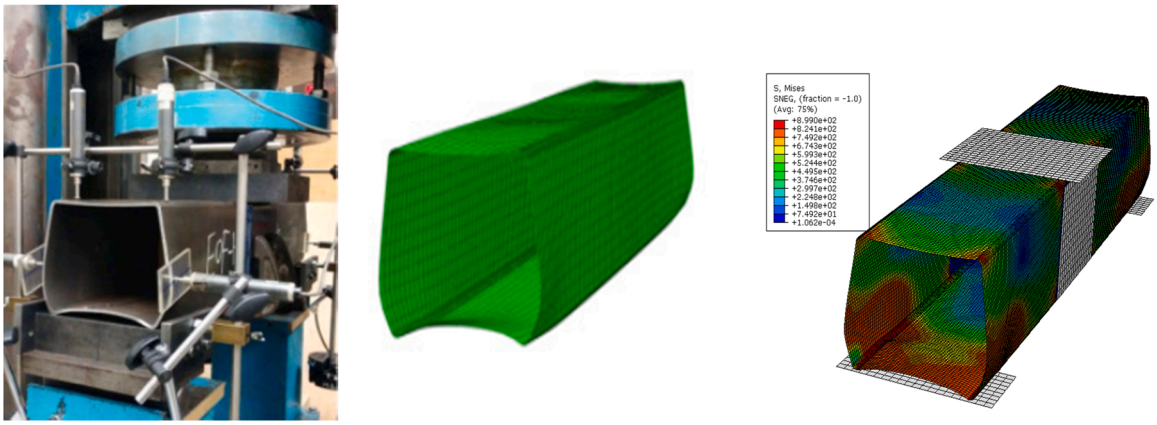

Fig. 6. Failure mode comparison of experimental vs FE-full model for the section H160 × 160 × 4N90.

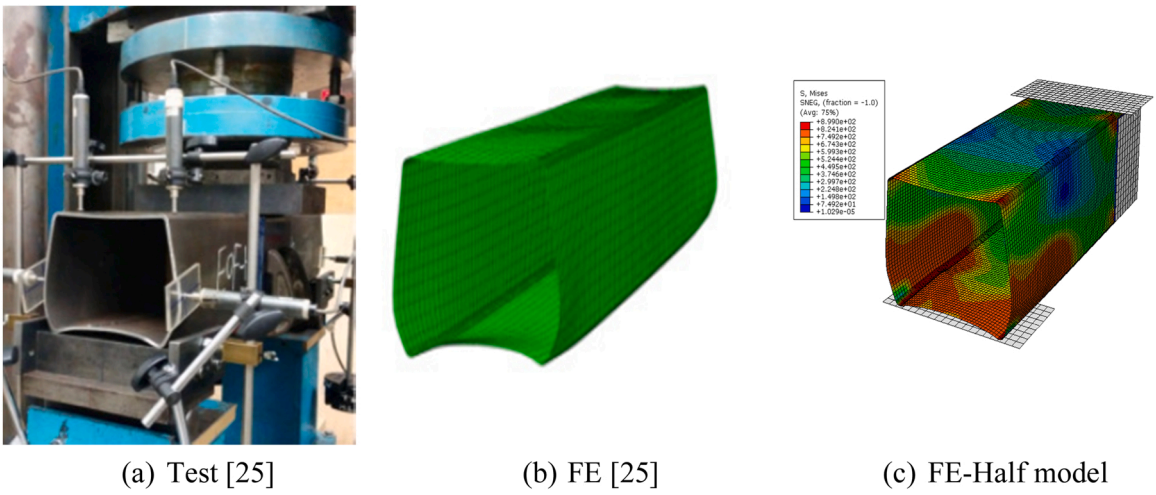

Fig. 7. Failure mode comparison of experimental vs FE-half model for the section H160 × 160 × 4N90.

Table 3
Detailed parametric study plan.

Section (d×b_f) (mm × mm)	Thickness (t) (mm)	Internal radius (r_i) (mm)	Bearing length (N) (mm)	Yield strength (f_y) (MPa)	Young's modulus (MPa)	Poisson ratio	Material Density (kg/m^3)	No. of models
150 × 60	4, 6, 8	12, 15, 18	50, 100, 150	50, 100, 150	203,000	0.3	7850	81
200 × 75	4, 6, 8	12, 15, 18	50, 100, 150	50, 100, 150	203,000	0.3	7850	81
250 × 85	4, 6, 8	12, 15, 18	50, 100, 150	50, 100, 150	203,000	0.3	7850	81
Total								243

Note: d = overall depth of the section and b_f = width of the flange.

5. Results

This section discusses the web crippling results of high-strength unlipped channel section under EOF loading condition. Table 4 presents the detailed ultimate web crippling capacity of high-strength CFS unlipped channel sections. Fig. 9 shows the applied load vs displacement curve for the section 150 × 60 (t = 8 mm, r_i = 12 mm, N = 150 mm and f_y = 1000 MPa) and corresponding web crippling failure progression is clearly illustrated in Fig. 10 in terms of initial-stage, before-ultimate stage, ultimate stage and post ultimate stage. In the parametric study, various geometrical parameters including section dimensions, thicknesses, internal radii, and

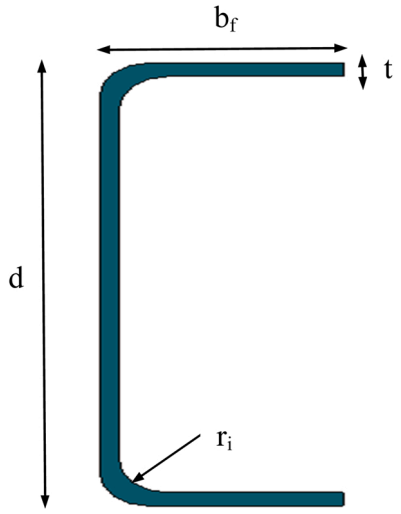

Fig. 8. Section dimension of unlipped channel beam.

bearing lengths were considered to investigate the web crippling behaviour under EOF condition. The detailed effect of these parameters on the web crippling capacity of high-strength CFS unlipped channel sections are presented in the following sub-sections:

5.1. Effect of thickness (t) on the web crippling capacity

The effect of thickness of the section on the web crippling strength is shown in Fig. 11(a). It clearly depicts an increasing trend of web crippling strength of the sections when thickness increases. As the thickness (t) changed from 4 mm to 8 mm for the section 200 × 75 (r_i = 12 mm, N = 150 mm and f_y = 1000 MPa), it is observed that the web crippling strength of the section increased from 55.69 kN to 248.64 kN shown in the Fig. 11(b). It means the web crippling strength of thickness 8 mm sections shows 346.47% greater than the thickness of 4 mm sections.

5.2. Effect of internal radius (r_i) on the web crippling capacity

Fig. 12(a) illustrates the effect of internal radius (r_i) of the section on the web crippling capacity, this graph shows that the downward trend of the web crippling strength when the internal radius of the section increases. From the parametric results, 124.99 kN and 108.59 kN are the web crippling capacity of the high-strength unlipped channel section 200 × 75 (t = 6 mm, N = 100 mm and f_y = 1000 MPa) when the internal radius (r_i) of the section increases from 12 mm to 18 mm (Fig. 12(b)), respectively. Also, which clearly depicts that the decrease in strength about 13.12%.

5.3. Effect of bearing length (N) on the web crippling capacity

When the bearing length of the loading plate higher, the web crippling capacity of the unlipped channel sections shows increment. Fig. 13(a) gives the effect of bearing length on the web crippling behaviour of the beams. From the FE results, it is observed that the web crippling capacity of the section 150 × 60 (t = 6 mm, r_i = 15 mm and f_y = 900 MPa) is 91.14 kN for bearing length 50 mm and 133.99 kN for bearing length 150 mm, which shows that the increase in strength about 47.02% is clearly illustrated in the Fig. 13(b).

6. Comparisons of FE results with current design guidelines

6.1. AS/NZS 4600 [29] and AISI S100 [8]

The design standards AS/NZS 4600 [21] and AISI S100 [8] for CFS structures specified identical design guidelines to determine the nominal web crippling capacity of the CFS sections. The specified equation is given by Eq. (11) which is used to predict the strength under the EOF load case. These design guidelines are adopted based on the detailed past experimental data analysis by Prabakaran and Schuster [6] and which is suitable to open CFS sections with different geometrical parameters. The design equation accounts the various parameters such as flat web portion to thickness (slenderness) ratio (d_1/t), bearing length to thickness ratio (N/t), internal radius to thickness ratio (r_i/t), strength of the material (f_y) and the angle of web surface plane to the flange surface plane (θ). Note that the parameters in the equation (Eq. (11)) should satisfy the following conditions such as $\frac{d_1}{t} \leq 200$, $\frac{N}{t} \leq 210$, $\frac{r_i}{t} \leq 2$, $\frac{N}{d_1} \leq 2$ and $\theta = 90^\circ$.

Table 4
Detailed parametric study results.

No.	Section ($d \times b_f$) (mm × mm)	Thickness (t)(mm)	Internal radius (r_i) (mm)	Bearing length (N) (mm)	Web crippling capacity (Rb) (kN)		
					fy = 700	fy = 900	fy = 1000
1	150 × 60	4	12	50	37.57	42.79	45.39
2	150 × 60	4	15	50	34.69	39.90	42.95
3	150 × 60	4	18	50	32.34	38.97	37.96
4	150 × 60	4	12	100	49.90	58.81	61.37
5	150 × 60	4	15	100	45.23	55.30	59.93
6	150 × 60	4	18	100	41.57	48.77	56.06
7	150 × 60	4	12	150	54.65	65.28	70.77
8	150 × 60	4	15	150	51.29	63.94	66.64
9	150 × 60	4	18	150	47.10	58.53	62.42
10	150 × 60	6	12	50	82.24	96.38	104.72
11	150 × 60	6	15	50	72.86	91.14	97.80
12	150 × 60	6	18	50	70.88	79.86	85.57
13	150 × 60	6	12	100	111.82	131.19	139.19
14	150 × 60	6	15	100	101.47	123.67	131.87
15	150 × 60	6	18	100	97.69	113.75	125.63
16	150 × 60	6	12	150	109.50	134.89	150.47
17	150 × 60	6	15	150	108.97	133.99	140.98
18	150 × 60	6	18	150	103.81	130.53	140.87
19	150 × 60	8	12	50	139.84	166.43	179.70
20	150 × 60	8	15	50	126.67	145.68	164.20
21	150 × 60	8	18	50	111.93	132.30	146.01
22	150 × 60	8	12	100	177.10	211.78	236.78
23	150 × 60	8	15	100	166.27	208.92	228.16
24	150 × 60	8	18	100	159.42	197.66	220.90
25	150 × 60	8	12	150	203.70	206.33	245.01
26	150 × 60	8	15	150	203.23	236.83	213.79
27	150 × 60	8	18	150	183.05	193.22	237.43
28	200 × 75	4	12	50	37.59	42.40	44.50
29	200 × 75	4	15	50	34.76	40.93	40.88
30	200 × 75	4	18	50	31.83	38.18	38.87
31	200 × 75	4	12	100	42.42	48.74	51.27
32	200 × 75	4	15	100	40.65	44.84	49.13
33	200 × 75	4	18	100	35.40	43.60	45.19
34	200 × 75	4	12	150	51.05	55.30	61.28
35	200 × 75	4	15	150	48.99	54.46	58.68
36	200 × 75	4	18	150	44.83	51.51	55.43
37	200 × 75	6	12	50	82.62	97.89	103.56
38	200 × 75	6	15	50	69.21	91.69	97.62
39	200 × 75	6	18	50	69.88	80.18	88.56
40	200 × 75	6	12	100	100.83	117.82	124.99
41	200 × 75	6	15	100	91.27	109.16	117.29
42	200 × 75	6	18	100	84.31	101.33	108.59
43	200 × 75	6	12	150	103.11	141.62	143.54
44	200 × 75	6	15	150	112.70	130.78	141.10
45	200 × 75	6	18	150	105.80	126.85	135.40
46	200 × 75	8	12	50	141.76	171.79	182.48
47	200 × 75	8	15	50	127.51	157.58	171.29
48	200 × 75	8	18	50	116.38	140.16	150.29
49	200 × 75	8	12	100	176.09	210.32	225.60
50	200 × 75	8	15	100	160.27	194.89	214.79
51	200 × 75	8	18	100	148.09	182.86	194.33
52	200 × 75	8	12	150	204.69	235.76	267.02
53	200 × 75	8	15	150	200.49	234.51	255.09
54	200 × 75	8	18	150	186.36	227.71	244.62
55	250 × 85	4	12	50	36.46	40.54	42.63
56	250 × 85	4	15	50	34.42	39.31	39.11
57	250 × 85	4	18	50	31.56	37.35	35.65
58	250 × 85	4	12	100	41.30	44.60	47.72
59	250 × 85	4	15	100	37.99	43.16	44.39
60	250 × 85	4	18	100	34.54	38.32	42.70
61	250 × 85	4	12	150	47.96	54.07	55.69
62	250 × 85	4	15	150	45.13	49.75	52.95
63	250 × 85	4	18	150	42.33	49.22	52.12
64	250 × 85	6	12	50	82.41	96.36	101.64
65	250 × 85	6	15	50	73.38	88.97	95.40
66	250 × 85	6	18	50	65.70	81.96	84.12
67	250 × 85	6	12	100	96.26	111.37	117.58

(*continued on next page*)

Table 4 (*continued*)

No.	Section (d×b_f) (mm × mm)	Thickness (t)(mm)	Internal radius (r_i) (mm)	Bearing length (N) (mm)	Web crippling capacity (Rb) (kN)		
					fy = 700	fy = 900	fy = 1000
68	250 × 85	6	15	100	87.62	102.41	111.11
69	250 × 85	6	18	100	79.30	97.87	103.26
70	250 × 85	6	12	150	110.43	130.40	141.19
71	250 × 85	6	15	150	104.88	126.22	131.86
72	250 × 85	6	18	150	100.25	124.90	124.74
73	250 × 85	8	12	50	144.24	170.31	181.39
74	250 × 85	8	15	50	128.69	149.68	167.15
75	250 × 85	8	18	50	115.18	129.10	151.85
76	250 × 85	8	12	100	172.62	210.07	218.07
77	250 × 85	8	15	100	157.72	191.67	204.39
78	250 × 85	8	18	100	147.51	162.84	189.91
79	250 × 85	8	12	150	212.57	238.07	248.64
80	250 × 85	8	15	150	205.35	226.58	244.52
81	250 × 85	8	18	150	185.24	223.58	231.17

Note: d = overall depth of the section and b_f = width of the flange.

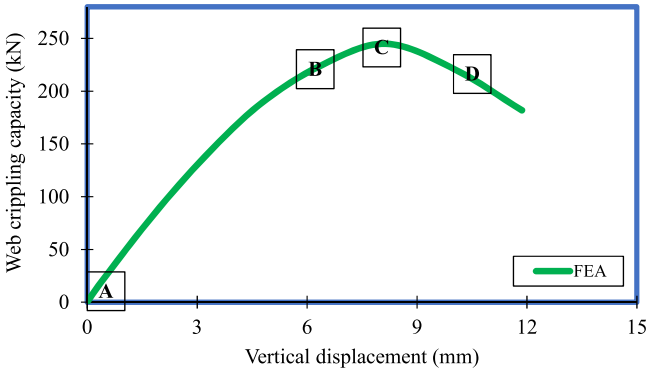

Fig. 9. Applied load vs displacement plot of section 150 × 60 with f_y of 1000 MPa.

$$R_{bAS/NZS4600} = Ct^2 f_y sin\theta\left(1 - C_R\sqrt{\frac{r_i}{t}}\right)\left(1 + C_N\sqrt{\frac{N}{t}}\right)\left(1 - C_h\sqrt{\frac{d_1}{t}}\right) \tag{11}$$

where f_y is the yield stress, t is the thickness of the section, d_1 is the height of the flat web portion, N is the bearing length, r_i is the inside corner radius and C, C_R, C_N and C_h are the geometrical coefficients for the CFS single web channel section with unfastened and unstiffened flange condition from AISI S100 Tables G5-2 [8] and AS/NZ 4600 Table 3.3.6.2(B) [21].

The results obtained from the FE analysis were compared with the design equation (Eq. (11)) of AS/NZS 4600 [21] and AISI S100 [8], shown in Fig. 14 The comparison results provided the mean and COV value as 1.04 and 0.24 respectively. The comparisons shows that the codified design guidelines were unsafe or unconservative to calculate the web crippling capacity of the high-strength unlipped channel sections under EOF condition.

6.2. *Eurocode 3 Part 1–3 [30]*

Eurocode 3 Part 1–3 [30] standard provides design guidelines for web crippling strength for CFS structures. The presented equations can predict the nominal web crippling capacity of CFS sections under transverse loading conditions (ETF, ITF, EOF and IOF). The mentioned design equations (Eq. (12)) can determine the web crippling strength of single unstiffened CFS section subjected to EOF load case and which is limited to the two conditions including $\frac{r_i}{t} \leq 6$ and, $\frac{h_w}{t} \leq 200$.

$$R_{bEC3} = \frac{k_1 k_2 k_3 f_y t^2}{\gamma_{M1}}\left[5.92 - \frac{h_w}{132t}\right]\left[1 + 0.01\frac{N}{t}\right] \tag{12}$$

where, $k_1 = 1.33 - 0.33\frac{f_y}{228}$, $k_2 = 1.15 - 0.15\frac{r_i}{t}$ $0.5 \leq k_2 \leq 1.0$, $k_3 = 0.7 - 0.3\left(\frac{\theta}{90}\right)^2$.

h_w is the web height between the midlines of the flanges, $\gamma_{M1} = 1$ is the partial safety factor and θ is the angle of web surface plan to

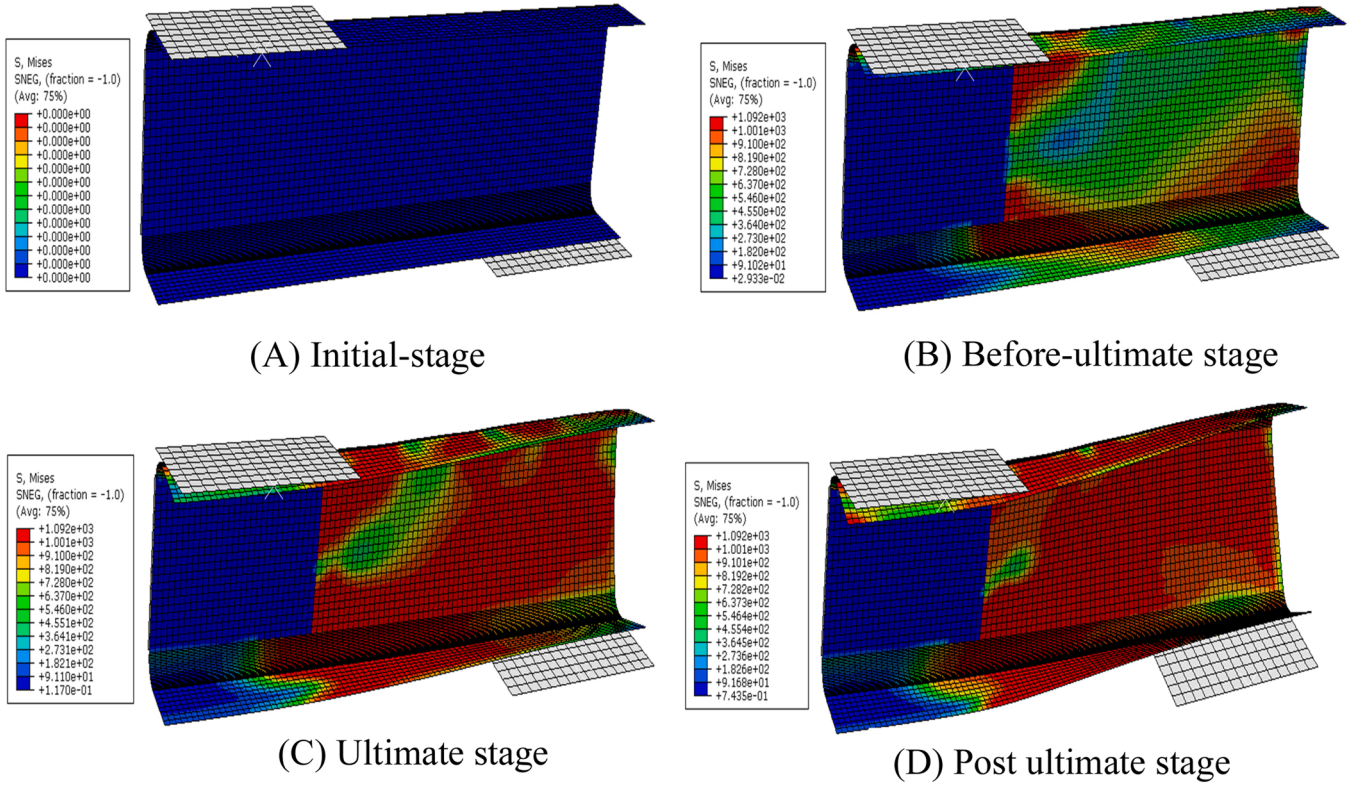

Fig. 10. Web crippling failure progression of section 150 × 60 with yield strength of 1000 MPa.

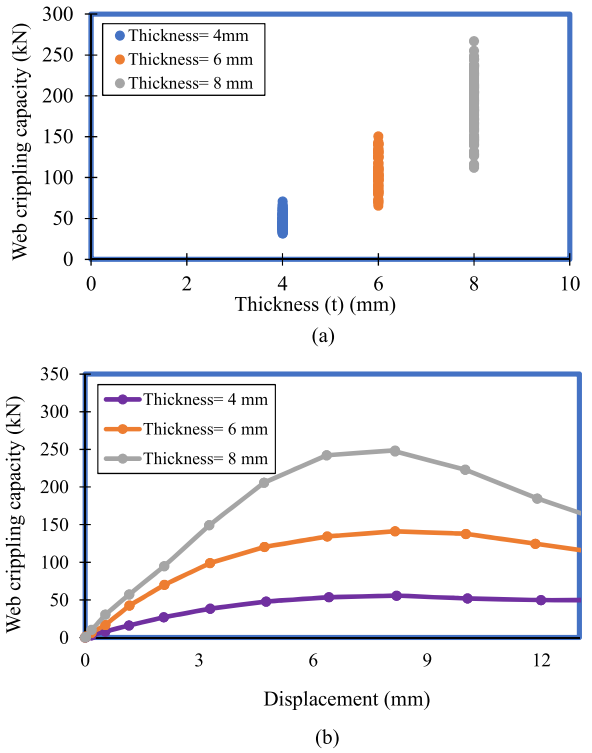

Fig. 11. (a) Effect of thickness (t) on the web crippling strength. (b) Load-displacement plot for the section 200 × 85 with varied thickness (t).

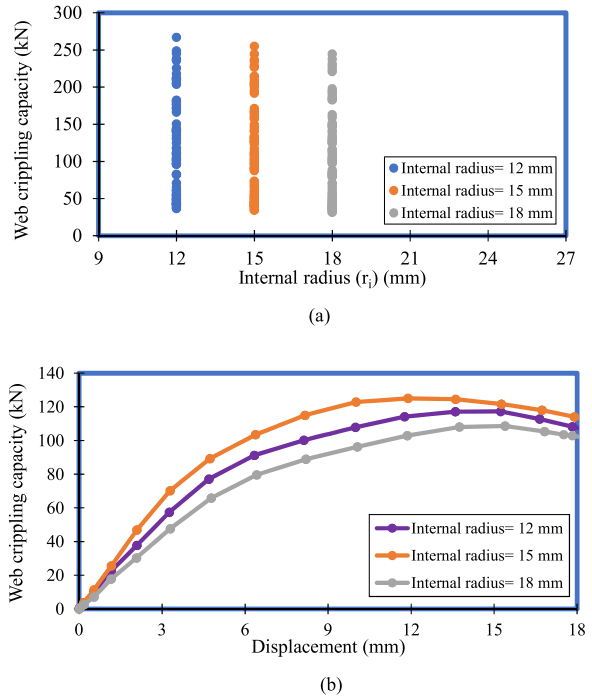

Fig. 12. (a) Effect of internal radius (r_i) of the section on the web crippling strength. (b) Load-displacement plot for the section 200 × 75 with varied internal radius (r_i).

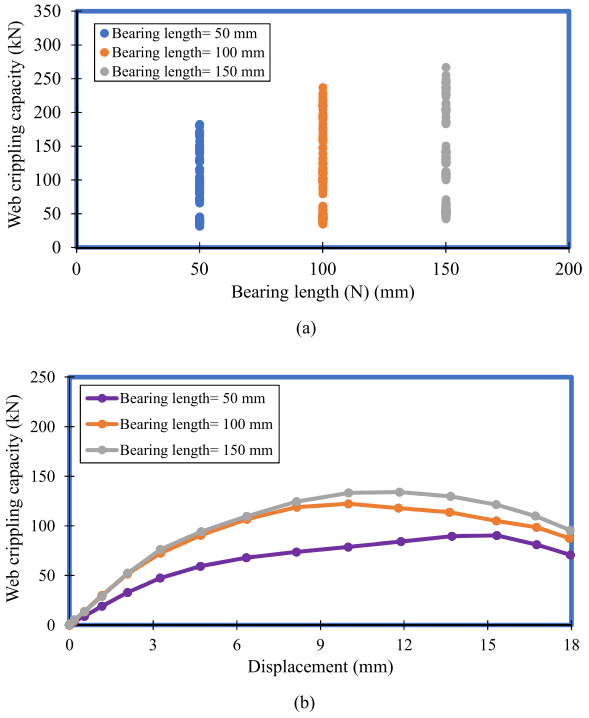

Fig. 13. (a) Effect of bearing length (N) on the web crippling strength. (b) Load-displacement plot for the section 150 × 60 with varied bearing length (N).

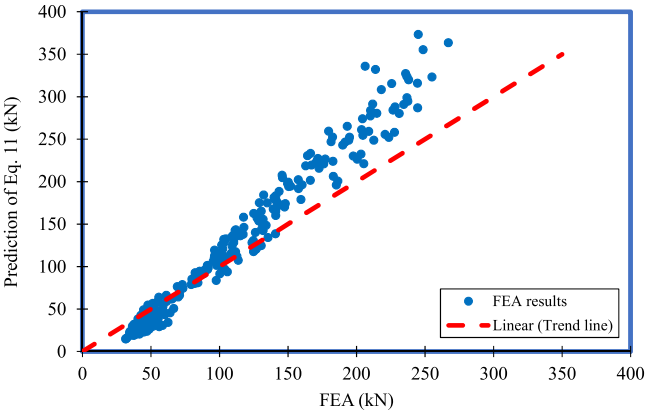

Fig. 14. Comparison of FEA results with AS/NZS 4600 [21] and AISI S100 [8].

the flange surface plane.

Fig. 15 illustrates the comparisons of available design equation (Eq. (12)) prediction results with the FEA data, the mean and COV value of the prediction results are 0.09 and 0.86. The comparison results clearly depicts that the design guidelines of Eurocode 3 Part 1–3 [30] is highly over conservative and unsafe for high-strength CFS beams. Moreover, it could be noted that the comparison result gave negative web crippling strength values for the sections with yield strength of 1000 MPa. Therefore, this comparisons neglected the FEA results of 1000 MPa strength sections and which clearly depicts that the design guidelines of Eurocode 3 [30] cannot be used to predict the web crippling capacity of unlipped channel sections with high-strength under EOF loading condition.

Even though AS/NZS 4600 [21] and AISI S100 [8] recommend a unified equation to predict the web crippling capacity with different coefficients by considering various cold-formed steel sections, all four loading conditions and supporting conditions, Eurocode 3 Part 1–3 [30] provide different design equations for each load cases. Moreover, Eurocode 3 Part 1–3 [30] does not categorise the supporting conditions. The AS/NZS 4600 [21] and AISI S100 [8] equations are developed based on experimental results of Prabakaran et al. [55]. Those experiments used different specimen lengths, test procedures and did not consider the higher yield strength of the material. Meanwhile, design rules available in the Eurocode 3 Part 1–3 [30] are developed based on the old AISI standard [56]. The

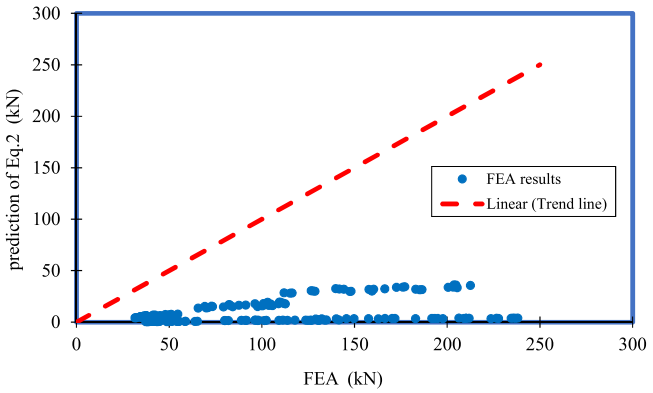

Fig. 15. Comparison of FEA results with Eurocode 3 [30].

design equations are not suitable for commercially available high-strength sections due to the inconsistencies of past researches and limitation of parametric in design standards.

6.3. *Sundararajah [57]*

Sundararajah [57] conducted extensive web crippling investigation on CFS sections using experimental and numerical simulation. Based on the design guidelines (Eq. (11)) of AS/NZS 4600 [21] and AISI S100 [8], the research study proposed improved coefficients to predict the web crippling capacity of unlipped channel sections under EOF loading condition. Comparison study was conducted between prediction using the improved design equation by Sundararajah [57] and FEA data. The mean and COV of the comparison were 1.60 and 0.16 respectively. Therefore, this proposed coefficients by Sundararajah [57] was unsafe or unconservative and not able to estimate the appropriate web crippling behaviour of high-strength unlipped channel beams under EOF condition. The comparison results illustrated in Fig. 16.

7. Proposed equations for high-strength unlipped channel section under EOF load case

7.1. *Proposed Eq. (1)*

The comparison results showed that the available design guidelines and equations were not feasible to determine the web crippling strength of high strength unlipped channel beams under EOF load case. Therefore, this study has proposed new improved coefficients (Eq. (13)) based on the AS/NZ 4600 [21] and AISI S100 [8] using extensive parametric results. To evaluate the accuracy level of proposed Eq. (1) (Eq. (13), the mean and COV values were 1.00 and 0.07 respectively. Therefore, the capacity reduction factor (φ_w) values is 0.90 for the proposed Eq. (1) (Eq. (13)) shown in the Table 5. Fig. 17 illustrates the plot of predicted results of proposed Eq. (1) (Eq. (13)) with FEA data, the comparison results shows that the proposed equation (Eq. (13)) has good agreement with parametric results and able to determine the appropriate web crippling strength of unlipped channel sections under EOF load case with unfastened flange condition.

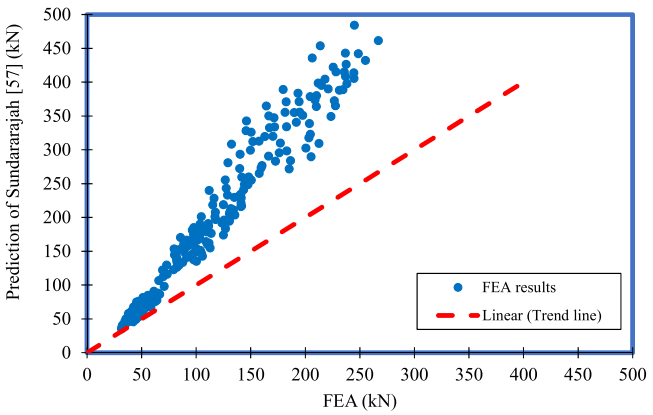

Fig. 16. Comparison of FEA results with Sundararajah [57].

Table 5
Reliability analysis of the proposed equations.

Proposed equations	Mean	COV	Reduction factor (φ_w)
Proposed Eq. (1) (Eq. (13))	1.00	0.07	0.90
Proposed Eq. (2) (Eq. (14))	1.00	0.05	0.91
Proposed DSM equations (Eqs. (23) and (24))	1.00	0.06	0.91

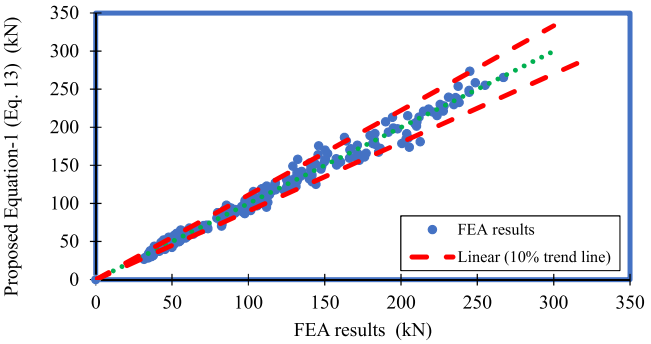

Fig. 17. Comparison plot of FEA results with proposed Eq. (1) (Eq. (13)).

$$R_b = 1.82t^2 f_y sin\theta\left(1 - 0.21\sqrt{\frac{r_i}{t}}\right)\left(1 + 0.61\sqrt{\frac{N}{t}}\right)\left(1 - 0.04\sqrt{\frac{d_1}{t}}\right) \tag{13}$$

7.2. Proposed Eq. (2)

The parametric results clearly show that the significant increasing of web crippling strength of the sections when the material strength changes from 700 MPa to 1000 MPa. Therefore, the new equation (Eq. (14)) incorporated with the strength factor (C_f) was developed using FEA results. It was observed that Eq. (14) resulted in higher level of accuracy compared to Eq. (13) due to the inclusion of addition strength. Mean, COV and capacity reduction factor (φ_w) value were calculated as 1.00, 0.05 and 0.91 respectively and illustrated in Table 5. The comparison of predicted results of proposed Eq. (2) with FEA data are illustrated in Fig. 18. The both proposed equations (Eqs. (13) and (14)) are highly recommended for the web crippling strength prediction of the high-strength unlipped channel beams under EOF load case with unfastened flange condition.

$$R_b = 0.54t^2 f_y sin\theta\left(1 - 0.21\sqrt{\frac{r_i}{t}}\right)\left(1 + 0.63\sqrt{\frac{N}{t}}\right)\left(1 - 0.03\sqrt{\frac{d_1}{t}}\right)\left(1 + 4.27\sqrt{\frac{250}{f_y}}\right) \tag{14}$$

8. Direct strength method

Direct-strength method is an another method to determine the capacity of CFS members developed by Schafer [58]. However, these DSM design equations were not included in the current design guidance AS/NZS 4600 [21], AISI S100 [8] and Eurocode 3 part 1–3

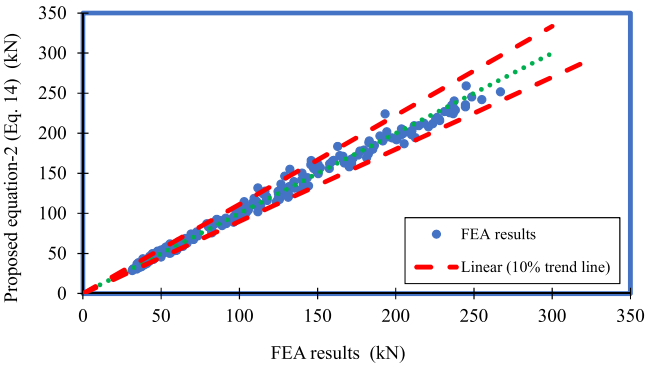

Fig. 18. Comparison plot of FEA results with proposed Eq. (2) (Eq. (14)).

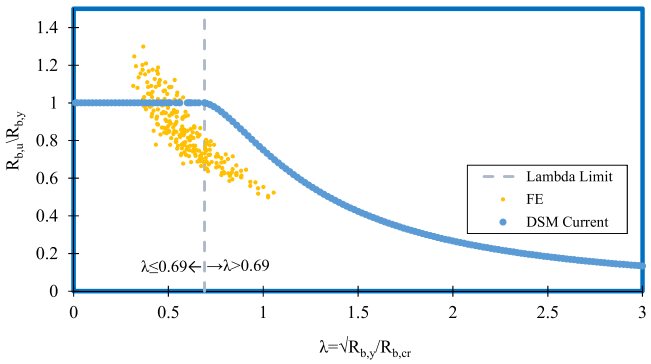

Fig. 19. Comparison between parametric results and available DSM equation [57].

[30] for web crippling. Many studies [17–19,26–29], developed suitable DSM design equations to predict the web crippling behaviour of CFS recently. Sundararajah et al. [57] proposed suitable DSM equations to predict the web crippling strength of CFS unlipped channel section under EOF loading conditions, given by Eqs. (15) and (16). The DSM approach was compared with FE results of this study to ensure the applicability. The comparison is presented by Fig. 19 and the mean and COV of comparison were 0.86 and 0.17 respectively for FEA results over prediction of DSM equations (Eqs. (15) and (16)). Therefore, Equations proposed by Sundararajah [57] is not suitable to predict the web crippling capacity of unlipped channel section with high-strength material.

$$\frac{R_b}{R_{b,y}} = 1 \quad for \quad \lambda \leq 0.69 \tag{15}$$

$$\frac{\mathrm{R_b}}{\mathrm{R_{b,y}}} = \left(1 - 0.25 \left(\frac{1}{\lambda}\right)^{0.90}\right)\left(\frac{1}{\lambda}\right)^{0.90} \text{for} \lambda > 0.69 \tag{16}$$

where, $\lambda = \sqrt{\frac{R_{b,y}}{R_{b,cr}}}$ is a slenderness ratio.

Following the comparison of available DSM equation, new DSM based equations were proposed. Critical buckling load ($R_{b,cr}$) and yield load ($R_{b,y}$) of unlipped channel section was calculated using Eqs. (17) and (18), respectively.

$$R_{b,cr} = \frac{k\pi^2 E t^3}{12(1-v^2)d} \tag{17}$$

$$R_{b,y} = f_y N_m \left(\sqrt{4{r_m}^2 + t^2} - 2r_m\right) \tag{18}$$

Supporting equations used to calculate the yield load ($R_{b,y}$) of unlipped channel section is illustrated by Eqs. (19)–(21).

$$N_m = \quad l_b + (2.5r_{ext} + 0.9d_1) \tag{19}$$

$$r_m = r_i + \frac{t}{2} \tag{20}$$

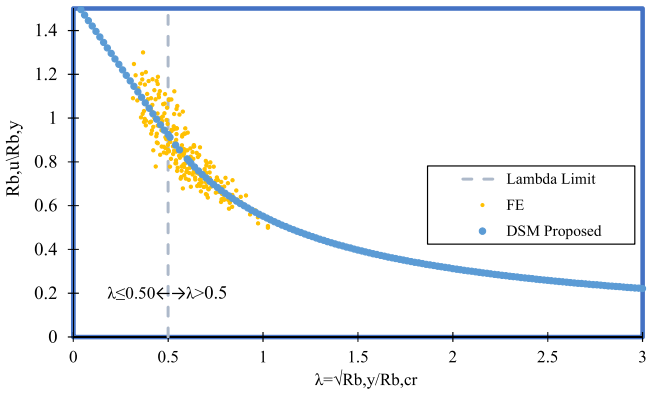

Fig. 20. Comparison between parametric results and proposed DSM equation.

$$r_{ext} = r_i + t \tag{21}$$

where, k is the buckling coefficient, E is modulus of elasticity, t is thickness, v is Poisson's ratio, N_m is the yield mechanism length, f_y is the yield stress, l_b is the bearing length, r_m is the internal bent radius at the middle of the section, r_{ext} is the internal bent radius of the outer section and d is the web height.

The buckling coefficient (k) was determined using Sundararajah [57] study on unlipped channel section (see Eq. (22)).

$$k = C_b\left(1 - C_{b,r}\sqrt{\frac{r_i}{t}}\right)\left(1 + C_{b,l}\sqrt{\frac{N}{t}}\right)\left(1 - C_{b,w}\sqrt{\frac{d1}{t}}\right)\left(1 + C_{b,b}\sqrt{\frac{b_f}{t}}\right) \tag{22}$$

where, C_b - general coefficient = 1.01, $C_{b,r}$ - Coefficient of inside bent radius to thickness ratio = 0.01, $C_{b,w}$ - Coefficient of web slenderness ratio = 0.4, $C_{b,l}$ - Coefficient of bearing length to thickness ratio = 0.05 and $C_{b,b}$ - Coefficient of flange width to thickness ratio = 0.01.

The developed DSM approach is given by Eqs. (23) and (24) whilst comparison of the proposed DSM vs FE results of unlipped channel section with high-strength under EOF loading condition is illustrated in Fig. 20. The comparison between proposed DSM and FE results showed the mean, COV and reduction factor (ϕ_w) values of 1.00, 0.06 and 0.91 respectively.

$$\frac{R_b}{R_{b,y}} = -1.25\lambda + 1.54 \quad for \quad \lambda \le 0.50 \tag{23}$$

$$\frac{R_b}{R_{b,y}} = 0.61\left(1 - 0.1\left(\frac{1}{\lambda}\right)^{0.89}\right)\left(\frac{1}{\lambda}\right)^{0.89} \quad for \quad \lambda > 0.50 \tag{24}$$

9. Reliability analysis

Reliability analysis was performed to evaluate the capacity reduction factors (φ_w) for the proposed equations. AISI S100 [8] provided the capacity reduction factor equation (Eq. (25)) and respective parameters. The parameters P_m and V_p are mean and COV values of FEA results to the predicted proposed equation values.

$$\varphi_w = 1.52 M_m F_m \quad P_m e^{-\beta_0} \quad \sqrt{\left\{V_m^2 + \quad V_f^2 + C_p V_p^2 + V_q^2\right\}} \tag{25}$$

where,

β_0 = reliability index, which is equal to 2.5.

M_m and V_m = mean and COV of the material factor, which are 1.1 and 0.1.

F_m and V_f = mean and COV of the fabrication factor, which are 1.0 and 0.05.

V_q = COV of load effect, which is equal to 0.21.

C_p = correction factor $\lfloor 1 + \frac{1}{n} \rfloor \lfloor \frac{m}{m-2} \rfloor$.

n = number of tests.

m = degree of freedom (m = n-1).

10. Conclusion

This paper investigated the web crippling behaviour of high-strength CFS unlipped channel sections subjected to the EOF load case with unfastened flange condition. High-strength CFS grades such as 700 MPa, 900 MPa and 1000 MPa were used in this study. Initially, a non-linear FE models were developed and validated against the available experiment results under EOF loading condition using ABAQUS software [47]. In the validation, both full and simplified half model analysis were performed and recommended FE-half models to carry out the parametric study with less computational time and higher accuracy in results. ABAQUS/Explicit solver was used in the numerical simulation study. In the extensive parametric FE investigation, 243 FE models were modelled and analysed with various key parameters such as web clear height to thickness ratio, internal radius to thickness ratio, bearing length to thickness ratio, section thickness and material yield strength to study web crippling behaviour of high-strength CFS unlipped channel beams. Based on the parametric results, the effect of section thickness (t = 4–8 mm) and bearing length (N = 50–150 mm) showed that the significant increase in average web crippling strength of the sections about 303.14% and 47.06% respectively. However, the average web crippling capacity was reduced about 12.08% due to the effect of internal radius (r_i = 12–18 mm).

The web crippling capacity obtained from the numerical analysis was compared with the available design guidelines such as AS/NZS 4600 [21] and AISI S100 [8], Eurocode 3 Part 1–3 [30] and Sundararajah [57] to check their suitability. The comparison study showed that the existing design standards AS/NZS 4600 [21] and AISI S100 [8] and Sundararajah [57] were unsafe or unconservative. Whilst, Eurocode 3 Part 1–3 [30] is highly over conservative and not able to predict the web crippling capacity of high strength CFS unlipped channel sections under EOF load case. Therefore, based on numerical results, improved design equations were developed according to the current design standards and new DSM based design equations were proposed. The capacity reduction factors were calculated using reliability analysis, which showed that the proposed design equations are capable of estimating the web crippling

strength of high strength CFS unlipped channel sections under EOF load case with high level of accuracy.

Declaration of Competing Interest

The authors declare that they have no known competing financial interests or personal relationships that could have appeared to influence the work reported in this paper.

Acknowledgements

The authors would like to acknowledge Northumbria University, The Home Engineers and European Research Council for massive support to conduct this research study.

References

[1] X. Meng, L. Gardner, Cross-sectional behaviour of cold-formed high strength steel circular hollow sections, Thin-Walled Struct. 156 (2020), 106822.
[2] J.L. Ma, T.M. Chan, B. Young, Material properties and residual stresses of cold-formed high strength steel hollow sections, J. Constr. Steel Res. 109 (2015) 152–165.
[3] J. Chen, T.M. Chan, Material properties and residual stresses of cold-formed high-strength-steel circular hollow sections, J. Constr. Steel Res. 170 (2020), 106099.
[4] AISI S909, Standard Test Method for Determining the Web Crippling Strength of Cold-formed Steel Beams, American Iron and Steel Institute, 2017.
[5] E. Kanthasamy, H. Alsanat, K. Pologanathan, P. Gatheeshgar, M. Corradi, K. Thirunavukkarasu, M. Dissanayake, Web Crippling Behaviour of Cold-formed Steel Unlipped Channel Beams with High-strength, Buildings 12 (3) (2022), 291.
[6] K. Prabakaran, R. Schuster, Web crippling of cold formed steel members, in: CCFSS Proceedings of the International Specialty Conference on Cold-Formed Steel Structures, 1998.
[7] R. Schuster, B. Beshara, Web Crippling Data and Calibrations of Cold Formed Steel Members, 2000.
[8] AISI S100, North American Specification for the Design of Cold-Formed Steel Structural Members, American Iron and Steel Institute, 2016, p. 78.
[9] B. Young, G.J. Hancock, Design of cold-formed channels subjected to web crippling, J. Struct. Eng. vol. 127 (10) (2001) 1137–1144.
[10] B. Young, G.J. Hancock, Cold-formed steel channels subjected to concentrated bearing load, J. Struct. Eng. 129 (8) (2003) 1003–1010.
[11] B. Young, G.J. Hancock, Web crippling of cold-formed unlipped channels with flanges restrained, Thin-Walled Struct. 42 (6) (2004) 911–930.
[12] W.X. Ren, S.E. Fang, B. Young, Finite-element simulation and design of cold-formed steel channels subjected to web crippling, J. Struct. Eng. 132 (12) (2006) 1967–1975.
[13] M. MacDonald, M.A. Heiyantuduwa Don, M. Kotełko, J. Rhodes, Web crippling behaviour of thin-walled lipped channel beams, Thin-Walled Struct. 49 (5) (2011) 682–690.
[14] M. MacDonald, M.A. Heiyantuduwa, A design rule for web crippling of cold-formed steel lipped channel beams based on nonlinear FEA, Thin-Walled Struct. 53 (2012) 123–130.
[15] Y. Chen, X. Chen, C. Wang, Experimental and finite element analysis research on cold-formed steel lipped channel beams under web crippling, Thin-Walled Struct. 87 (2015) 41–52.
[16] A.P.C. Duarte, N. Silvestre, A new slenderness-based approach for the web crippling design of plain channel steel beams, Int. J. Steel Struct. 13 (3) (2013) 421–434.
[17] P. Natário, N. Silvestre, D. Camotim, Direct strength prediction of web crippling failure of beams under ETF loading, Thin-Walled Struct. 98 (2016) 360–374.
[18] P. Natário, N. Silvestre, D. Camotim, Web crippling of beams under ITF loading: a novel DSM-based design approach, J. Constr. Steel Res. 128 (2017) 812–824.
[19] S. Gunalan, M. Mahendran, Web crippling tests of cold-formed steel channels under two flange load cases, J. Constr. Steel Res. 110 (2015) 1–15.
[20] S. Gunalan, M. Mahendran, Experimental study of unlipped channel beams subject to web crippling under one flange load cases, Adv. Steel Constr. 15 (2) (2019) 165–172.
[21] AS/NZS 4600, Australian/New Zealand Standard Cold-Formed Steel Structures, 2018.
[22] C. Santaputra, M.B. Parks, W.W. Yu, Web crippling strength of cold-formed steel beams, J. Struct. Eng. vol. 115 (10) (1989) 2511–2527.
[23] S. Wu, W. Yu, R.A. LaBoube, Strength of Flexural Members Using Structural Grade 80 of A653 steel (Web Crippling Tests), Civil Engineering Study 97–3, Cold-Formed Steel Ser. Third Prog. Report, Univ. Missouri-Rolla, Roll. Missouri, USA, 1997.
[24] H.T. Li, B. Young, Tests of cold-formed high strength steel tubular sections undergoing web crippling, Eng. Struct. 141 (2017) 571–583.
[25] H.T. Li, B. Young, Design of cold-formed high strength steel tubular sections undergoing web crippling, Thin-Walled Struct. 133 (2018) 192–205.
[26] L. Sundararajah, M. Mahendran, P. Keerthan, Web crippling experiments of high strength lipped channel beams under one-flange loading, J. Constr. Steel Res. 138 (2017) 851–866.
[27] L. Sundararajah, M. Mahendran, P. Keerthan, Numerical modeling and design of lipped channel beams subject to web crippling under one-flange load cases, J. Struct. Eng. 145 (10) (2019) 04019094.
[28] L. Sundararajah, M. Mahendran, P. Keerthan, Experimental studies of lipped channel beams subject to web crippling under two-flange load cases, J. Constr. Steel Res. 142 (9) (2016) 04016058.
[29] L. Sundararajah, M. Mahendran, P. Keerthan, New design rules for lipped channel beams subject to web crippling under two-flange load cases, Thin-Walled Struct. 119 (2017) 421–437.
[30] EN 1993-1-3: Eurocode 3: Design of Steel Structures – Part 1–3: General Rules – Supplementary Rules for Cold-formed Members and Sheeting, 2006.
[31] B. Janarthanan, M. Mahendran, S. Gunalan, Bearing capacity of cold-formed unlipped channels with restrained flanges under EOF and IOF load cases, Steel Constr. 8 (3) (2015) 146–154.
[32] B. Janarthanan, M. Mahendran, S. Gunalan, Numerical modelling of web crippling failures in cold-formed steel unlipped channel sections, J. Constr. Steel Res. 158 (2019) 486–501.
[33] L. Sundararajah, M. Mahendran, P. Keerthan, Design of SupaCee sections subject to web crippling under one-flange load cases, J. Struct. Eng. 144 (12) (2018) 04018222.
[34] L. Sundararajah, M. Mahendran, P. Keerthan, Web crippling studies of SupaCee sections under two flange load cases, Eng. Struct. 153 (2017) 582–597.
[35] M. Almatrafi, M. Theofanous, M. Bock, S. Dirar, Slenderness-based design for sigma sections subjected to interior one flange loading, Thin-Walled Struct. 158 (2021), 107194.
[36] P. Gatheeshgar, et al., Web crippling of slotted perforated cold-formed steel channels under EOF load case: simulation and design, J. Build. Eng. 44 (2021), 103306.
[37] P. Gatheeshgar, H. Alsanat, K. Pologanathan, S. Gunalan, N. Degtyareva, I. Hajirasouliha, Web crippling behaviour of slotted perforated cold-formed steel channels: IOF load case, J. Constr. Steel Res. 188 (2022), 106974.
[38] A. Uzzaman, J.B.P. Lim, D. Nash, K. Roy, Web crippling behaviour of cold-formed steel channel sections with edge-stiffened and unstiffened circular holes under interior-two-flange loading condition, Thin-Walled Struct. 154 (2020), 106813.

[39] A. Uzzaman, J.B.P. Lim, D. Nash, K. Roy, Cold-formed steel channel sections under end-two-flange loading condition: Design for edge-stiffened holes, unstiffened holes and plain webs, Thin-Walled Struct. 147 (2020), 106532.
[40] Z. Fang, K. Roy, Q. Ma, A. Uzzaman, J.B.P. Lim, Application of deep learning method in web crippling strength prediction of cold-formed stainless steel channel sections under end-two-flange loading, Structures 33 (2021) 2903–2942.
[41] B. Chen, K. Roy, Z. Fang, A. Uzzaman, Y. Chi, J.B.P. Lim, Web crippling capacity of fastened cold-formed steel channels with edge-stiffened web holes, unstiffened web holes and plain webs under two-flange loading, Thin-Walled Struct. 163 (2021), 107666.
[42] Z. Fang, et al., Numerical simulation and design recommendations for web crippling strength of cold-formed steel channels with web holes under interior-one-flange loading at elevated temperatures, Buildings 11 (12) (2021) 666.
[43] Z. Fang, K. Roy, Y. Chi, B. Chen, J.B.P. Lim, Finite element analysis and proposed design rules for cold-formed stainless steel channels with web holes under end-one-flange loading, Structures 34 (2021) 2876–2899.
[44] Z. Fang, K. Roy, A. Uzzaman, J.B.P. Lim, Numerical simulation and proposed design rules of cold-formed stainless steel channels with web holes under interior-one-flange loading, Eng. Struct. 252 (2022), 113566.
[45] M.J. Russell, J.B.P. Lim, K. Roy, G.C. Clifton, J.M. Ingham, Welded steel beam with novel cross-section and web openings subject to concentrated flange loading, Structures 24 (2020) 580–599.
[46] B. Janarthanan, L. Sundararajah, M. Mahendran, P. Keerthan, S. Gunalan, Web crippling behaviour and design of cold-formed steel sections, Thin-Walled Struct. 140 (2019) 387–403.
[47] Dassault Systems Simulia Corp, Abaqus/CAE 2017 User's Guide, Abaqus/CAE Standard, 2017.
[48] L. Gardner, X. Yun, Description of stress-strain curves for cold-formed steels, Constr. Build. Mater. 189 (2018) 527–538.
[49] E. Mirambell, E. Real, On the calculation of deflections in structural stainless steel beams: an experimental and numerical investigation, J. Constr. Steel Res. 54 (1) (2000) 109–133.
[50] B. Rossi, S. Afshan, L. Gardner, Strength enhancements in cold-formed structural sections — part II: predictive models, J. Constr. Steel Res. 83 (2013) 189–196.
[51] P. Gatheeshgar, K. Poologanathan, S. Gunalan, I. Shyha, K.D. Tsavdaridis, M. Corradi, Optimal design of cold-formed steel lipped channel beams: combined bending, shear, and web crippling, Structures 28 (2020) 825–836.
[52] K. Thirunavukkarasu, et al., Web crippling design of modular construction optimised beams under ETF loading, J. Build. Eng. 43 (2021), 103072.
[53] P. Natário, N. Silvestre, D. Camotim, Web crippling failure using quasi-static FE models, Thin-Walled Struct. 84 (2014) 34–49.
[54] J. Balasubramaniam, Structural Behaviour and Design of Cold-formed Steel Floor Systems (Ph.D. thesis), Queensland University of Technology, Brisbane, Australia, 2017.
[55] K. Prabakaran, R. Schuster, Web Crippling of Cold-formed Steel Sections, Project Report, Department of Civil Engineering, University of Waterloo, Ontario, Canada, 1993.
[56] AS/NZS 4600, Australia/New Zealand Standard for Cold-formed Steel Structures, Sydney, Australia, 1996.
[57] L. Sundararajah, Web Crippling Studies of Cold-formed Steel Channel Beams (Experiments, Numerical Analyses and Design Rules) (Ph.D. thesis) Queensland University of Technology, Brisbane, Australia, 2017.
[58] B.W. Schafer, Review: the direct strength method of cold-formed steel member design, J. Constr. Steel Res. 64 (7–8) (2008) 766–778.